Self-assembly *via* hydrogen bonding of bis(18-crown-6)-1,3-distyrylbenzene and [2 + 2] photocycloaddition: Stereoselective synthesis of [2.2] metacyclophanes and butterfly-type thermal isomerization

Timofey P. Martyanov [a,b,*], Artem P. Vorozhtsov [a,b], Evgeny N. Ushakov [a,b], Nikita A. Slesarenko [a], Ilia V. Sulimenkov [d], Sergey P. Gromov [b,c,**]

[a] Federal Research Center of Problems of Chemical Physics and Medicinal Chemistry, Russian Academy of Sciences, Chernogolovka, Moscow Region, 142432, Russian Federation
[b] NRC "Kurchatov Institute", Kurchatov Complex of Crystallography and Photonics, Photochemistry Center, Novatorov str. 7A-1, Moscow, 119421, Russian Federation
[c] Department of Chemistry, Lomonosov Moscow State University, Leninskie Gory 1-3, Moscow, 119991, Russian Federation
[d] Chernogolovka Branch of the N.N. Semenov Federal Research Center for Chemical Physics, Russian Academy of Sciences, Chernogolovka, Moscow Region, 142432, Russian Federation

ARTICLE INFO

ABSTRACT

The photochemistry of bis(18-crown-6)-containing 1,3-distyrylbenzene and its 2 : 2 bis-pseudo-sandwich complex with ethane-1,2-diammonium was studied. The UV irradiation of the supramolecular complex resulted in the formation of three geometric isomers of tetracrown-containing dicyclobutano[2.2]metacyclopane, differing in the orientation of the cyclobutane moieties, with the unsymmetrical isomer (>50 %) predominating. The diammonium cations used as the template could be removed after photolysis by simple extraction, and the product was obtained in high yield (82 %). The ^1H NMR signals of a mixture of geometric isomers of [2.2] metacyclophane derivative were assigned resorting to quantum chemistry methods (DFT). The kinetic and thermodynamic parameters of thermal isomerization between the *endo,endo-* and *exo,exo*-isomers were measured. Tetracrown-containing dicyclobutano[2.2]metacyclophanes are homotetratopic ligands that contain four binding sites for metal and ammonium cations, which is of interest for the design of photo- and thermo-switchable supramolecular devices with a variable complex formation behavior and supramolecular machines owing to the butterfly-type thermal isomerization.

1. Introduction

Cyclophanes are bridged aromatic compounds that can efficiently bind neutral and charged molecules to give host–guest complexes; therefore, they can be used to design molecular recognition systems [1–4]. Functionalized cyclophanes can be used to model membrane channels [5] and enzymes [6] and for the development of optically active catalysts [7]. The incorporation of cyclophanes into polymer backbones and side chains may endow macromolecules with new optical, electronic, and topological properties [8,9]. Chemical synthesis of low-molecular-weight cyclophanes requires the use of additional reagents [10–12] some of which can be unsafe (BuLi, selenocyanides). One

more approach to the synthesis of cyclophanes is the use of [2 + 2]-photocycloaddition (PCA) reaction of distyrylbenzene derivatives; however, because of side electrocyclization reactions, this approach does not provide high purity of the products and gives mixtures of cyclophanes with significant amount of fused cyclic products [13,14].

Previously, we performed the self-assembly of crown-containing stilbene derivatives through hydrogen bonding and obtained bis-ligand complexes using the alkanediammonium ions $^+H_3N(CH_2)_nNH_3^+$ (**A**n^{2+}), where n = 2–4 [15–18]. The supramolecular pre-organization dramatically increased the quantum yield of PCA and provided for stereospecificity. When diammonium salts are used to assemble crown compounds, the template can be easily removed after photocyclization

by simple extraction. In the case of PCA in pseudo-sandwich (18-crown-6)stilbene complexes (*E*)-**S**, the reaction had a moderate quantum efficiency [17,18]. but it was stereospecific and gave cyclobutane derivative as only one *rctt*-isomer (Scheme 1). The addition of the second crown ether moiety into the molecule sharply (almost 50-fold) increased the PCA quantum yield; however, photolysis of bis-ligand complexes ((*E*)-**BCS**)$_2$·(**A***n*$^{2+}$)$_2$ gave 1,2,3,4-tetra(benzo-18-crown-6) cyclobutane as a mixture of *rctt*- and *rtct*-isomers in which the former predominated [15,16].

We assumed that our approach would also be applicable to distyrylbenzene derivatives. In this study, a similar template, ethane-1,2-diammonium perchlorate (**A2**(ClO$_4$)$_2$), was used for the photochemical synthesis of tetracrown-containing [2.2]metacyclophane from bis (18-crown-6)-1,3-distyrylbenzene (*E*,*E*)-**DSB**. Owing to the crown ether moieties, the resulting [2.2]metacyclophane derivative is simultaneously a host molecule for two types of guests, metal and ammonium cations. These compounds may be of interest as photo- and thermoactive supramolecular devices (machines) with a controlled complexation function, and they can also be used to design coordination polymers or metal-organic frameworks [19,20].

The first photochemical synthesis of [2.2]metacyclophane was performed by irradiating a concentrated solution of unsubstituted 1,3-distyrylbenzene [21]. As a result of chromatographic purification, the target product was obtained in 59 % yield as a mixture of three isomers, from which the pure unsymmetrical isomer was later isolated. The use of supramolecular pre-organization for the photochemical synthesis of cyclophanes was first proposed in our study [22]. In Ref. [23], *exo*, *exo*-dicyclobutano-[2.2]metacyclophane was photochemically obtained as the only isomer in the crystalline phase from 2 : 2 associates of 1,3-di (vinyl-γ-pyridyl)benzene with 4-chlororesorcinol (template).
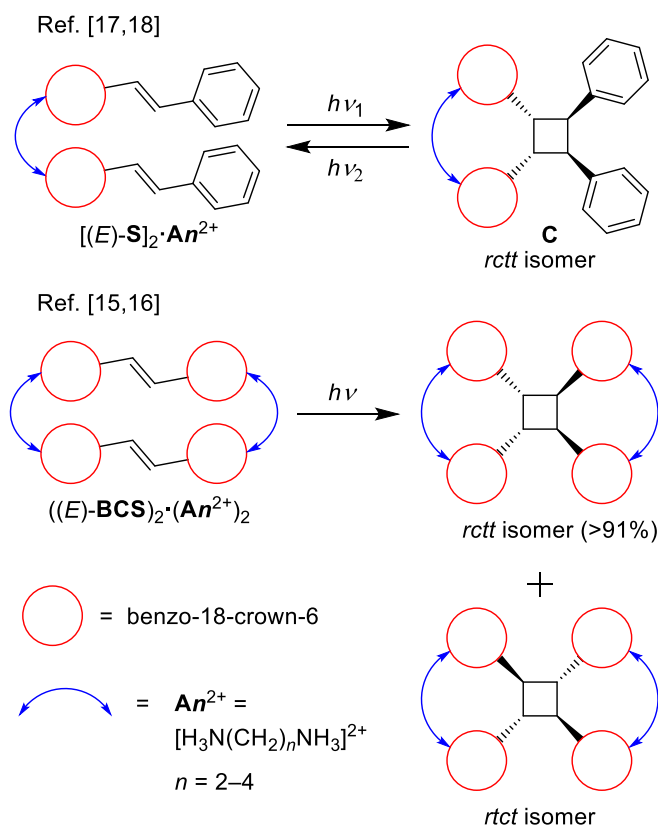
Scheme 1. Our previous works.

2. Results and discussion

The bis-crown 1,3-distyrylbenzene (*E*,*E*)-**DSB** was obtained according to the method described in Ref. [24]. The ligand **DSB** can be useful in the following areas: optical chemosensors for Cs$^+$, the selectivity of which is based on the tweezer effect [25], photocontrollable ion extraction [26] and design of supramolecular charge-transfer complexes [27,28].

2.1. Complex formation

The complexation of bis-crown (*E*,*E*)-**DSB** with ethanediammonium perchlorate **A2**(ClO$_4$)$_2$ in solution was studied by spectrophotometry and NMR spectroscopy. A quantum chemical calculation performed earlier [24] demonstrated that unsymmetrical conformation (*E*,*E*)-**DSB** predominates in solution.

The addition of ethanediammonium perchlorate to a solution of (*E*, *E*)-**DSB** in MeCN induces a blue shift of the long-wavelength absorption band by 4 nm (Fig. 1). This attests to the interaction of the **A2**$^{2+}$ ammonioalkyl groups with the crown ether oxygen atoms of (*E*,*E*)-**DSB**.

When a small amount of the **A2**(ClO$_4$)$_2$ salt is added to the solution, two equilibria can exist (Scheme 2).

The equilibria depicted in Scheme 2 can be written in the following way:

$$L + A \overset{K_1}{\rightleftarrows} L \cdot A, \tag{1}$$

$$2 L \cdot A \overset{K_2}{\rightleftarrows} (L)_2 \cdot (A)_2, \tag{2}$$
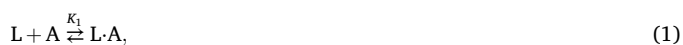
where L and A are distyrylbenzene (*E*,*E*)-**DSB** and ethanediammonium **A2**$^{2+}$, respectively, L·A is their 1:1 complex, (L)$_2$·(A)$_2$ is the 2:2 bis-pseudo-sandwich complex, and K_1 and K_2 are the stability constants of L·A and (L)$_2$·(A)$_2$, respectively.

Slight cation-induced spectral changes were observed during the spectrophotometric titration (SPT) (Fig. 1); hence, the absorption spectra of the complexes of different stoichiometry differ little. The approximation of SPT data by one equilibrium (1) using the parameterized matrix modeling method [29,30] was satisfactory, which is indicative of some linear correlation of the concentrations. Therefore, a simplified complex formation scheme was used:
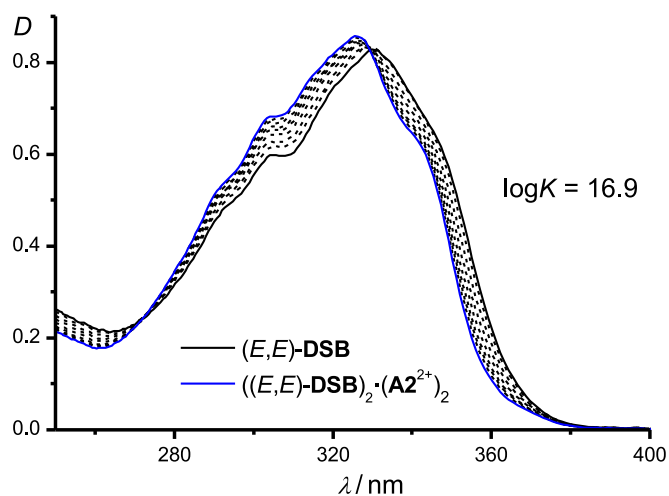

Fig. 1. Absorption spectra of the (*E*,*E*)-**DSB**–**A2**(ClO$_4$)$_2$ system in MeCN (1-cm cell) with the ligand concentration being constant (1.6 × 10^{-5} M) and the ethanediammonium perchlorate concentration (**A2**(ClO$_4$)$_2$) being varied in the range from 0 to 1.0 × 10^{-4} M. The ionic strength of the solution $I = 0.01$ M. The blue curve is the absorption spectrum of ((*E*,*E*)-**DSB**)$_2$·(**A2**$^{2+}$)$_2$ calculated by model (3).
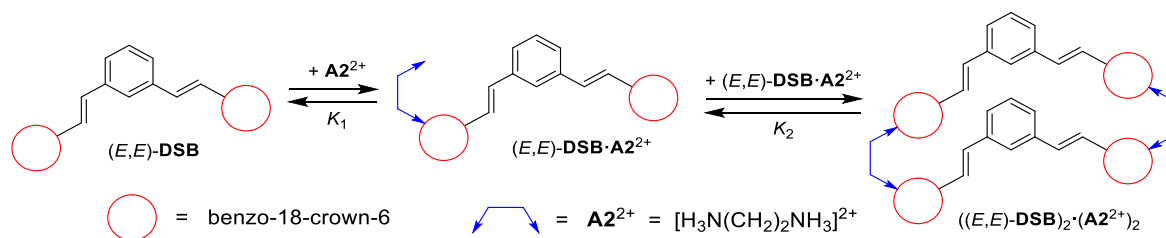
Scheme 2. Complexation of (E,E)-**DSB** with **A2**$^{2+}$.

$$2L + 2A \overset{K}{\rightleftharpoons} (L)_2 \cdot (A)_2. \qquad (3)$$

The stability constant K was determined on the basis of SPT data (Fig. 1) using equilibrium (3) to be 7.70×10^{16} M^{-1} (log$K = 16.9$). Using the law of mass action for equilibria (1) and (2), it is possible to derive the following expressions:

$$[L \cdot A] = K_1[L][A],$$

$$[(L)_2 \cdot (A)_2] = K_2[L \cdot A][L \cdot A].$$

After substitution of the first expression into the second one, one gets

$$[(L)_2 \cdot (A)_2] = K_2(K_1[L][A])^2 = K_2 K_1^2[L]^2[A]^2,$$

that is, the constant K in the simplified complex formation scheme (3) amounts to $K_2 K_1^2$. Then the dimerization constant K_2 is $7.70 \times 10^{16}/K_1^2$. The two styryl moieties in (E,E)-**DSB** occur in the *meta*-positions relative to each other; therefore, the conjugation between them is low. Hence, (18-crown-6)stilbene (E)-**S** can serve as the model compound. Therefore, the stability constant of (E)-**S**·**A2**$^{2+}$ measured previously (6.54×10^4 M^{-1}) was used as K_1 [17]. By substituting this value, we found the dimerization constant K_2 to be 1.8×10^7 M^{-1} (log$K_2 = 7.26$). The high K_2 value allows the synthesis of 2:2 bis-pseudosandwich complexes of (E,E)-**DSB** with **A2**$^{2+}$ virtually in a pure state (the partial concentration of the complex >0.99) at a slight excess of the diammonium salt in dilute solutions.

The reaction of (E,E)-**DSB** with **A2**$^{2+}$ was also studied by NMR spectroscopy (Figs. S2–S5 in ESI). The addition of an equimolar amount of **A2**(ClO$_4$)$_2$ to a solution of (E,E)-**DSB** in MeCN-d_3 induces a considerable broadening of ^{1}H NMR signals for the 1,3-distyrylbenzene derivative spectrum and a downfield shift of signals of aromatic and ethylene protons. The absence of shielding of some protons in the ((E,E)-**DSB**)$_2$·(**A2**$^{2+}$)$_2$ complex is probably caused by the shift of aromatic moieties of the ligand in the complex relative to each other, as a result of which the protons do not fall into the shielding area.

A study of an equimolar mixture of (E,E)-**DSB** and **A2**(ClO$_4$)$_2$ by electrospray ionization mass spectrometry (Fig. S35) did not provide unambiguous evidence for the presence of ((E,E)-**DSB**)$_2$·(**A2**$^{2+}$)$_2$ complexes in solution. However, the spectrum did show the signals for the [**DSB** + **A2**-H]$^+$ and [2 × **DSB** + **A2**]$^{2+}$ ions.

2.2. Photochemistry of the free ligand

The irradiation of a solution of crown-containing 1,3-distyrylbenzene (E,E)-**DSB** in MeCN at $\lambda = 313$ or 365 nm (Fig. 2) leads to a considerable decrease in the long-wavelength absorption band (330 nm) and a shift of the absorption maximum to shorter wavelength (280 nm). The observed spectral changes correspond to E–Z photoisomerization of stilbene derivatives (Scheme 3, Fig. S6).

Long-term photoirradiation induces a slight increase in the absorption intensity in the 370–400 nm range, which is probably due to the side formation of crown-containing fused aromatic compounds upon electrocyclization reactions of Z-isomers of **DSB**.

Measurement of the quantum yields of E–Z photoisomerization of **DSB** in air-saturated solutions is a challenging task. For obtaining reliable data, it is necessary to know the absorption spectrum of (E,Z)-**DSB**. However, it is difficult to isolate the mixed isomer. Nevertheless, using global analysis of spectral data [29,30], Fischer method [31], and the spectra of the quasi-photostationary states (Fig. 3, S39), it is possible to roughly estimate the quantum yields for the first step of E–Z photoisomerization (φ_{EZ} and φ_{ZE}). It is noteworthy that the start of photolysis is accompanied by a sharp decrease in the absorbance at the absorption maximum (Fig. S39). In the case of irradiation at 313 nm, this period lasts for up to ~100 s, after which the slope of the kinetic curve decreases, which attests to the presence of two photoprocesses (formation of (E,Z)-**DSB** and (Z,Z)-**DSB**).

Since one styryl moiety has a slight effect on the other one (the absorption maxima of the *trans*-isomers of **DSB** and **S** are close to each other), the E–Z photoisomerization of one styryl moiety of (E,E)-**DSB** should not have a considerable effect on the φ_{EZ} value of the second
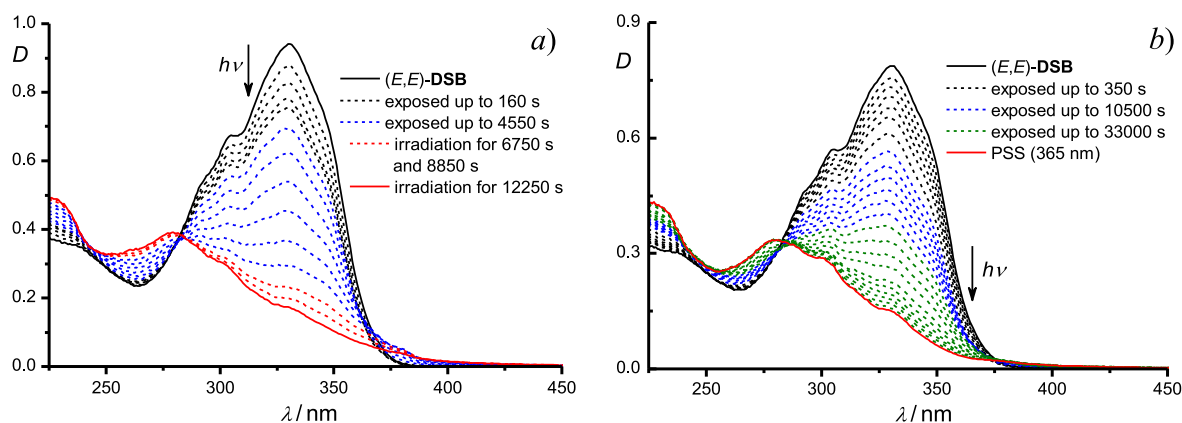
Fig. 2. Spectrophotometric data for steady-state photolysis of (E,E)-**DSB** in MeCN, 1 cm cell: (*a*) irradiation wavelength $\lambda = 313$ nm, (E,E)-**DSB** concentration of 1.8×10^{-5} M, light intensity $I_{act} = 2.3 \times 10^{-9}$ mol cm^{-2}·s^{-1}; (*b*) irradiation wavelength $\lambda = 365$ nm, (E,E)-**DSB** concentration of 1.5×10^{-5} M, light intensity $I_{act} = 1.9 \times 10^{-9}$ mol cm^{-2}·s^{-1}.
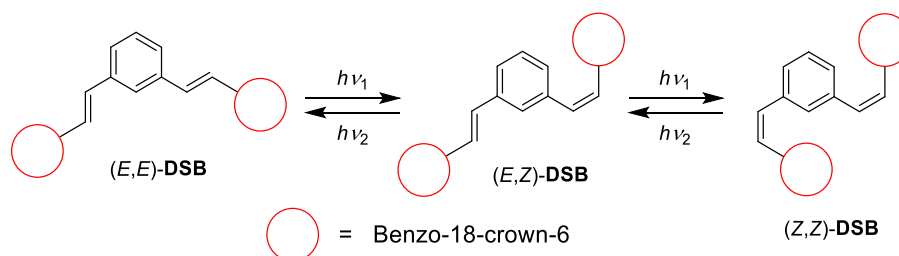
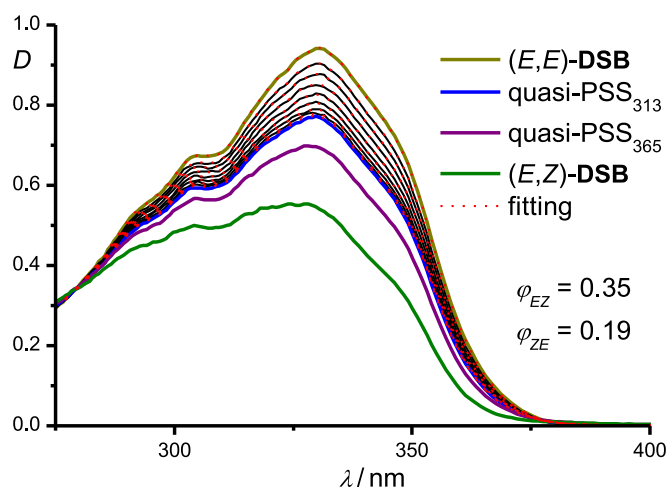**Scheme 3.** Photoconversions of crown-containing 1,3-distyrylbenzene.

Fig. 3. Spectrophotometric data for the steady-state photolysis of (*E,E*)-**DSB** at 313 nm: MeCN, 1 cm cell, $C(\mathbf{DSB}) = 1.8 \times 10^{-5}$ M, light intensity $I_{act} = 2.3 \times 10^{-9}$ mol cm^{-2}·s^{-1}. The green curve is the spectrum of (*E,Z*)-**DSB** calculated using the Fischer approximation. The red dots designate the absorption spectra calculated using the kinetic equation for reversible unimolecular photoreactions with quantum yields for the forward (φ_{EZ}) and reverse (φ_{ZE}) reactions being 0.35 and 0.19, respectively.

moiety.

The quantum yield of the forward *E–Z* photoisomerization of (*E,E*)-**DSB** proved to be somewhat lower than that for (18-crown-6)stilbene (*E*)-**S** (Table 1). Apparently, this is due to increased rate of intersystem crossing for distyrylbenzene (*E,E*)-**DSB** and, as a consequence, a relatively high yield of triplet states [33]. Attention is attracted by the quantum yield of the *Z–E* photoisomerization for (*E,Z*)-**DSB**, which is twice lower than the analogous quantum yield for (*Z*)-**S**. The latter almost does not fluoresce, unlike (*E,Z*)-**DSB**, in which the styryl moiety occurs in the *E*-configuration and which probably has a considerable contribution of the radiative deactivation of the S_1 state.

Table 1
Spectral characteristics of the photoisomers of crown compounds **S** and **DSB** and *E–Z* photoisomerization quantum yields.[a]

	S	DSB
λ_{max}^E/nm	326	331
$\varepsilon_{max}^E \times 10^{-3}$/M^{-1} cm^{-1}	29.4	52.5
λ_{max}^Z/nm	291	327
$\varepsilon_{max}^Z \times 10^{-3}$/M^{-1} cm^{-1}	10.3	30.8
φ_{EZ}	0.39	0.35
φ_{ZE}	0.40	0.19

[a] In MeCN, the error of measurement of quantum yields is ±30 %. The data for **S** were taken from Ref. [32]. The presented data for (*Z*)-**DSB** refer to the mixed (*E,Z*)-isomer of **DSB**.

2.3. Photochemistry of bis-pseudo-sandwich complex

Long-term photoirradiation of an equimolar mixture of (*E,E*)-**DSB** and **A2**(ClO$_4$)$_2$ in MeCN at $\lambda = 313$ nm gives rise to new signals in the ^{1}H NMR spectrum of the photolysis products (Fig. S16). In particular, six multiplets with similar integrated intensity appear in the region of cyclobutane protons (4.2–4.8 ppm) (Fig. 4); they can be assigned to complexes formed by geometric isomers of *rctt*-[2.2]metacyclophane derivatives **MC**·(**A2**$^{2+}$)$_2$. These isomers may include *endo,endo*-, *exo,exo*- and *endo,exo*-isomers, which differ from one another by the relative spatial orientation of the cyclobutane moieties (Scheme 4). The unsymmetrical *endo,exo*-**MC**·(**A2**$^{2+}$)$_2$ is present in the greatest amount. The ^{1}H NMR spectra were assigned resorting to the results of quantum chemical calculations (see Chapter 2.4.).

A low-intensity singlet is present at 9.83 ppm; together with the signals at 6.9–7.8 ppm, this is indicative of the formation of 4′-formylbenzo-18-crown-6 ether (<5 %). The photolysate virtually does not show signals at 8–9 ppm, indicating the absence (<1 %) of products of photoinduced electrocyclic reactions, that is, derivatives of fused aromatic compounds such as phenanthrene or tetraphene. Photolysis of a similar solution with the same light, but over a shorter period of time, results in the appearance of signals for (*E,Z*)-**DSB** and distyrylcyclobutane (*E*)-**DSC** in the ^{1}H NMR spectrum of the photolysate (Figs. S7 and S8). The latter compound gives rise to a characteristic doublet with a maximum at 4.44 ppm (Fig. S8). Thus, the products obtained upon photolysis attest to *E–Z* photoisomerization and PCA (two steps), which are depicted in Scheme 4.

The preparative photolysis produced **MC** derivatives in amounts

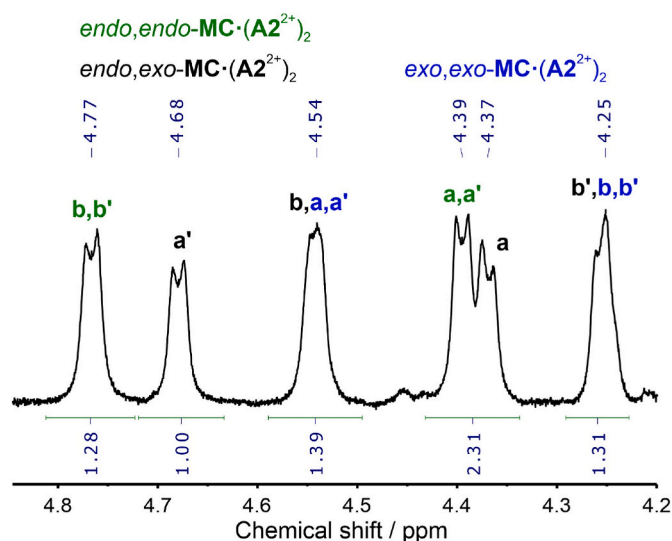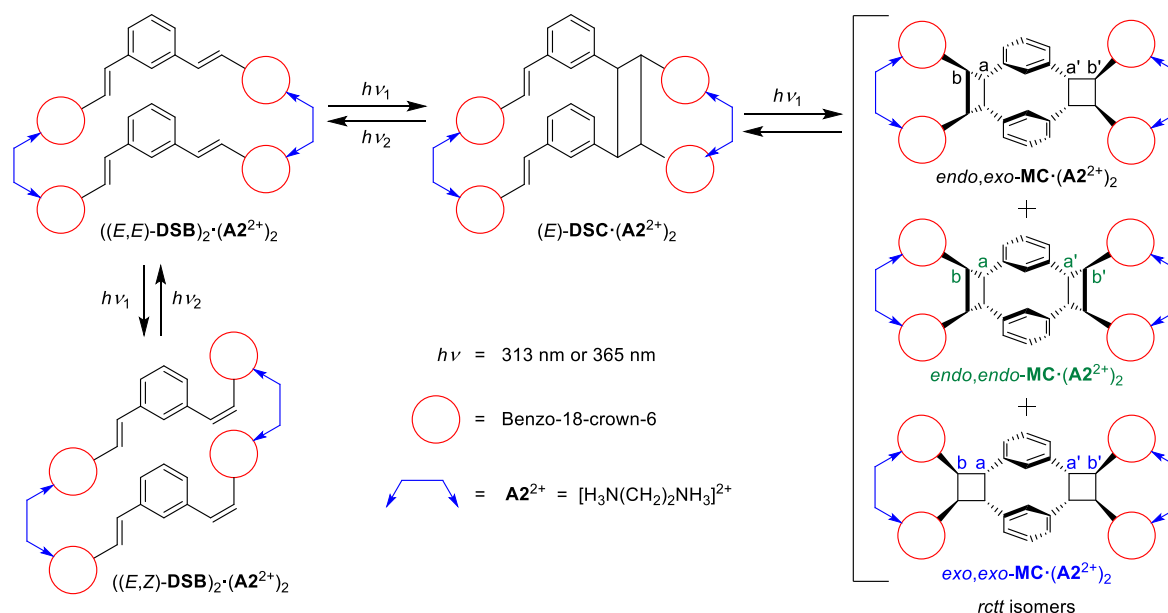**Fig. 4.** ^{1}H NMR (DMSO-d_6, 296 K, cyclobutane proton region) spectrum of the photolysate obtained from a mixture of (*E,E*)-**DSB** (1.5×10^{-3} M) and **A2** (ClO$_4$)$_2$ (1.5×10^{-3} M) in MeCN by irradiation with light at 313 nm wavelength for 4 h.

Scheme 4. Key photoreactions proceeding in the ((E,E)-**DSB**)$_2$·(**A2**$^{2+}$)$_2$ complex.

sufficient for the study. The diammonium salt was removed from the photolysate by simple extraction; the product yield was 82 %. The structures of the obtained cyclic **MC** products were confirmed not only by NMR data but also by mass spectrometry (Fig. S37). We failed to isolate individual **MC** isomers using recrystallization and TLC. For the latter, we used SiO$_2$ and Al$_2$O$_3$ plates and polar eluents (DMF, MeCN, acetone etc.) without or with perchloric acid additives. The tetracrown-containing [2.2]metacyclophanes **MC** formed a strong complex with the sorbent of TLC plates. It is noteworthy that the ratio of geometric isomers in solution changes after the photochemical synthesis of **MC** (Table 2, Fig. S27): the fraction of *endo,endo*-**MC** substantially decreases, while the content of *exo,exo*-**MC** increases. However, this does not occur immediately, but takes three weeks.

The irradiation of a solution of ((E,E)-**DSB**)$_2$·(**A2**$^{2+}$)$_2$ in MeCN with a monochromatic light at $\lambda = 313$ and 365 nm (Fig. 5) caused a dramatic drop of the absorbance in the long-wavelength spectral region, which was greater than that observed upon photolysis of free distyrylbenzene (E,E)-**DSB** (Fig. 2).

The absorption maximum observed in the spectrum after long-term irradiation (>10000 s) of complex ((E,E)-**DSB**)$_2$·(**A2**$^{2+}$)$_2$ at $\lambda = 313$ nm is 280 nm; in combination with the low absorption coefficient, this attests to the formation of [2.2]metacyclophane **MC** derivatives (Scheme 4). The absorbance in the 380–420 nm range does not grow, which implies the absence of fused aromatic by-products in the photolysis of

Table 2
Percentages of geometric isomers of [2.2]metacyclophane **MC** depending on the conditions of photolysis.[a]

Conditions	*endo,exo*-MC	*endo,endo*-MC	*exo,exo*-MC
365 nm (LED), −14 °C	54	42	3
365 nm (LED), 20–25 °C	50	38	12
365 nm (LED), 35 °C	55	29	16
365 nm (Hg)	54	29	17
313 nm (Hg)	53	35	12
After salt extraction [b]	53	11	36

[a] Equimolar mixtures of (E,E)-**DSB** (1.5×10^{-3} M) and **A2**(ClO$_4$)$_2$ (1.5×10^{-3} M) in 2 ml MeCN were irradiated; photolysates were evaporated and dissolved in 0.5 mL of DMSO-d_6; the product composition was determined from ^{1}H NMR spectroscopy data; the type of light source used (LED or mercury lamp) is indicated in parentheses.
[b] Composition for pure **MC** in DMSO-d_6 after reaching equilibrium.

the bis-pseudo-sandwich complex. It is worth noting that, along with two successive [2 + 2] photocycloaddition reactions (Scheme 4), photoirradiation may induce E–Z photoisomerization of both the starting complex and cyclobutane derivative (E)-**DSC**·(**A2**$^{2+}$)$_2$.

Photolysis of the bis-ligand complex at $\lambda = 365$ nm also leads to the disappearance of the long-wavelength absorption band (Fig. 5b). No absorption of the final products, [2.2]metacyclophanes **MC**, should be present at the irradiation wavelength. The complexes that absorb light in this region include the (E,E)-**DSB**, (Z,E)-**DSB**, and (E)-**DSC** complexes with the **A2**$^{2+}$ ions. Therefore, the quantum yields were measured on the basis of kinetic data obtained using monochromatic light at $\lambda = 365$ nm. The ^{1}H NMR spectrum of the photolysate formed after short-term irradiation (15 min, $\lambda_{ir} = 365$ nm) indicates that E–Z photoisomerization and PCA reaction giving cyclobutane (E)-**DSC** occur in parallel (Figs. S9 and S10). The content of (Z,E)-**DSB** relative to the starting (E,E)-**DSB** was 18 %, and that of (E)-**DSC** was 48 %. This means that the quantum yield of PCA is much higher than that of E–Z photoisomerization in ((E,E)-**DSB**)$_2$·(**A2**$^{2+}$)$_2$. Due to the difficulty of recording the spectra of (Z,E)-**DSB** complexes with **A2**$^{2+}$, the E–Z photoisomerization was neglected in the calculation of the quantum yields of the first (φ_{PCA1}) and second (φ_{PCA2}) PCA steps. The kinetics of photolysis can be described by a system of two differential equations:

$$dc_{EE}/dt = (\varphi_{\text{r-PCA1}}\varepsilon_{CB}c_{CB} - \varphi_{PCA1}\varepsilon_{EE}c_{EE})I_{act}F, \qquad (4)$$

$$dc_{CB}/dt = (\varphi_{PCA1}\varepsilon_{EE}c_{EE} - \varphi_{\text{r-PCA1}}\varepsilon_{CB}c_{CB} - \varphi_{PCA2}\varepsilon_{CB}c_{CB})I_{act}F, \qquad (5)$$

where I_{act} is the actinic light intensity, $F = (1-10^{-D})/D$, D is the absorbance of the solution at the irradiation wavelength (λ_{ir}), $\varphi_{\text{r-PCA1}}$ is the quantum yield of retro-PCA reaction of complex (E)-**DSC**·**A2**$^{2+}$, c_{EE} is the total partial concentration of (E,E)-**DSB**, ε_{EE} is the molar absorption coefficient of ((E,E)-**DSB**)$_2$·(**A2**$^{2+}$)$_2$ divided by 2, c_{CB} and ε_{CB} are the partial concentration and the molar absorption coefficient of complex (E)-**DSC**·**A2**$^{2+}$. The absorbance of the solution can be represented as $D = D_{EE} + D_{CB}$, where D_{EE} is the absorbance of complex ((E,E)-**DSB**)$_2$·(**A2**$^{2+}$)$_2$ at λ_{ir}, D_{CB} is the absorbance of complex (E)-**DSC**·**A2**$^{2+}$ at λ_{ir}. The calculated kinetic curves for the particular components of the mixture and the measured quantum yields are shown in Fig. 6. During photolysis, the partial concentration of the starting bis-ligand complex exponentially decreases, while that of complex **MC**·(**A2**$^{2+}$)$_2$ increases. The kinetic curve for distyrylcyclobutane (E)-**DSC**·**A2**$^{2+}$ has a maximum,
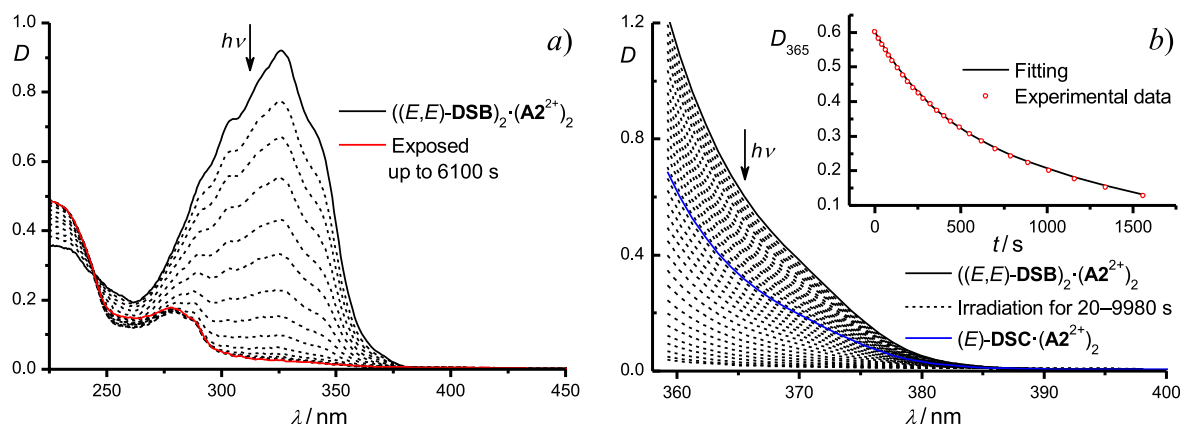
Fig. 5. Spectrophotometric data for the steady-state photolysis of complex $((E,E)$-**DSB**$)_2 \cdot ($**A2**$^{2+})_2$ in MeCN, 1 cm cell: (*a*) irradiation wavelength $\lambda_{ir} = 313$ nm, $I_{act} = 2.33 \times 10^{-9}$ mol cm$^{-2} \cdot$s^{-1}, (E,E)-**DSB** concentration of 1.73×10^{-5} M, **A2**(ClO$_4$)$_2$ concentration of 3.0×10^{-5} M, $I = 0.01$ M; (*b*) irradiation wavelength $\lambda_{ir} = 365$ nm, $I_{act} = 4.50 \times 10^{-9}$ mol cm$^{-2} \cdot$s^{-1}, (E,E)-**DSB** concentration of 1.71×10^{-4} M, **A2**(ClO$_4$)$_2$ concentration of 2.5×10^{-4} M, $I = 0.01$ M. The blue curve is the calculated spectrum of cyclobutane (E)-**DSC**$\cdot($**A2**$^{2+})_2$; the inset shows the approximation of the kinetic curve by equations (4) and (5).
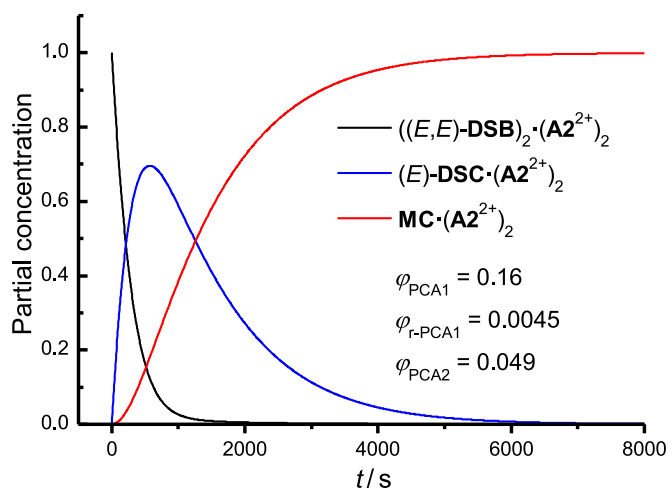
Fig. 6. Partial concentrations of complex $((E,E)$-**DSB**$)_2 \cdot ($**A2**$^{2+})_2$, cyclobutane derivative (E)-**DSC**$\cdot($**A2**$^{2+})_2$, and metacyclophanes **MC**$\cdot($**A2**$^{2+})_2$ derived from the kinetics of photolysis of the starting complex at $\lambda = 365$ nm by solving kinetic equations (4) and (5) with the quantum yields presented in the Figure.

which is to be expected.

The obtained φ_{PCA1} (0.16) value is lower than that for analogous complex of bis(18-crown-6)stilbene ($\varphi_{PCA} = 0.27$) [16]; however, it is high for this type of photoreactions. In the case of (18-crown-6)stilbene (one coordination site), the effective quantum yield of PCA in the bis-ligand complex with **A2**$^{2+}$ is 0.0057 [17,18], which is more than an order of magnitude lower than that for $((E,E)$-**DSB**$)_2 \cdot ($**A2**$^{2+})_2$. The quantum yield of the second PCA step ($\varphi_{PCA2} = 0.049$) is almost three times less than φ_{PCA1}. Since the calculation was carried out based on the number of reacted molecules, for a correct comparison we multiply the second value φ_{PCA2} by two. In this case, φ_{PCA1} exceeds φ_{PCA2} by only 60 %, which can be explained by a change in the orientation of the double bonds in the second styryl moiety after the first PCA step. The performed estimation of the quantum yields for two PCA reactions takes into account the reversibility of the first PCA reaction in complex $((E, E)$-**DSB**$)_2 \cdot ($**A2**$^{2+})_2$. If retro-PCA (φ_{r-PCA1}) is neglected, then $\varphi_{PCA1} = 0.16$ and $\varphi_{PCA2} = 0.047$ with a similar standard deviation.

As factors influencing the composition of a mixture of geometric isomers of [2.2]metacyclophane **MC** formed photochemically from complex $((E,E)$-**DSB**$)_2 \cdot ($**A2**$^{2+})_2$, we evaluated the effect of the irradiation wavelength and solution temperature on the photolysis (Table 2).

The change in the irradiation wavelength of photolysis from 313 nm

to 365 nm induces a slight decrease in the content of *endo,endo*-**MC** and some increase in the content of *exo,exo*-**MC**. In general, the wavelength and the type of irradiation source have little effect on the resulting mixture of the **MC** geometric isomers. An increase in the solution temperature in the photolysis of complex $((E,E)$-**DSB**$)_2 \cdot ($**A2**$^{2+})_2$ leads to a decrease in the proportion of *endo,endo*-**MC** and a parallel increase in the proportion of *exo,exo*-**MC**. It is noteworthy that the isomer ratio obtained upon LED irradiation at a temperature of -14 °C is very close to that obtained for unsubstituted 1,3-distyrylbenzene [21]. The effect of temperature can be attributed to a change in the ratio of conformations of the starting complex $((E,E)$-**DSB**$)_2 \cdot ($**A2**$^{2+})_2$ pre-organized towards the formation of particular geometric isomers of **MC**$\cdot($**A2**$^{2+})_2$.

The photoirradiation of a mixture of free metacyclophanes **MC** in MeCN solutions with LED light with a maximum emission at 275 nm for 1580 s induced an increase in the absorbance over a broad range (240–370 nm) (Fig. S41). The maximum in the long-wavelength part of the spectrum was at 328 nm, indicating the formation of a mixture of (E, E)-**DSB** and (E,Z)-**DSB** isomers of the starting 1,3-distyrylbenzene. The conversion of metacyclophanes **MC** to the starting distyrylbenzene **DSB** was less than 25 % provided that only (E,E)-isomer was formed. In the case of longer irradiation times (4300 and 8300 s), the pattern of the absorption spectrum considerably changed: the absorption intensity in the 320–345 nm range decreased, while those in the short- and long-wavelength regions increased. Long-term photolysis of **MC** with high-energy light might induce the formation of electrocyclic reaction products and fused aromatic compounds. Similar spectral changes were induced by irradiation of complex **MC**$\cdot($**A2**$^{2+})_2$ with the same light (275 nm, LED). Therefore, the two-step PCA reaction in complex $((E,E)$-**DSB**$)_2 \cdot ($**A2**$^{2+})_2$ can be considered reversible.

2.4. Density functional theory (DFT) calculations

The correctness of assignment of ^{1}H NMR signals for the geometric isomers of metacyclophane **MC** was verified by DFT calculations including the solvent (MeCN). For model cyclobutane *rctt*-**C** (Scheme 1), four conformers (Fig. S42) differing in the orientation of the crown ether substituent relative to the C(cyclobutane)–C(aryl) single bond were constructed: *s-trans,trans*, *s-cis,cis*, *s-trans,cis*, and *s-cis,trans*. Four C_2-symmetrical (or quasi-symmetrical in the case of *endo,exo*-**MC**) conformers were obtained on the basis of these structures for each **MC** isomer.

The *s-trans,cis*-rotamer was the lowest-energy conformer for each **MC** isomer (Table S1). Their structures are depicted in Fig. 7. In the case of cyclobutane *rctt*-**C**, the *s-trans,cis*-rotamer is also most favorable in energy (Table S2). Note that for each **MC** isomer, the conformers are close

*endo,endo-(s-trans,cis)-**MC***

*exo,exo-(s-trans,cis)-**MC***

*endo,exo-(s-trans,cis)-**MC***

⬤ — C   🔴 — O   🔵 — H
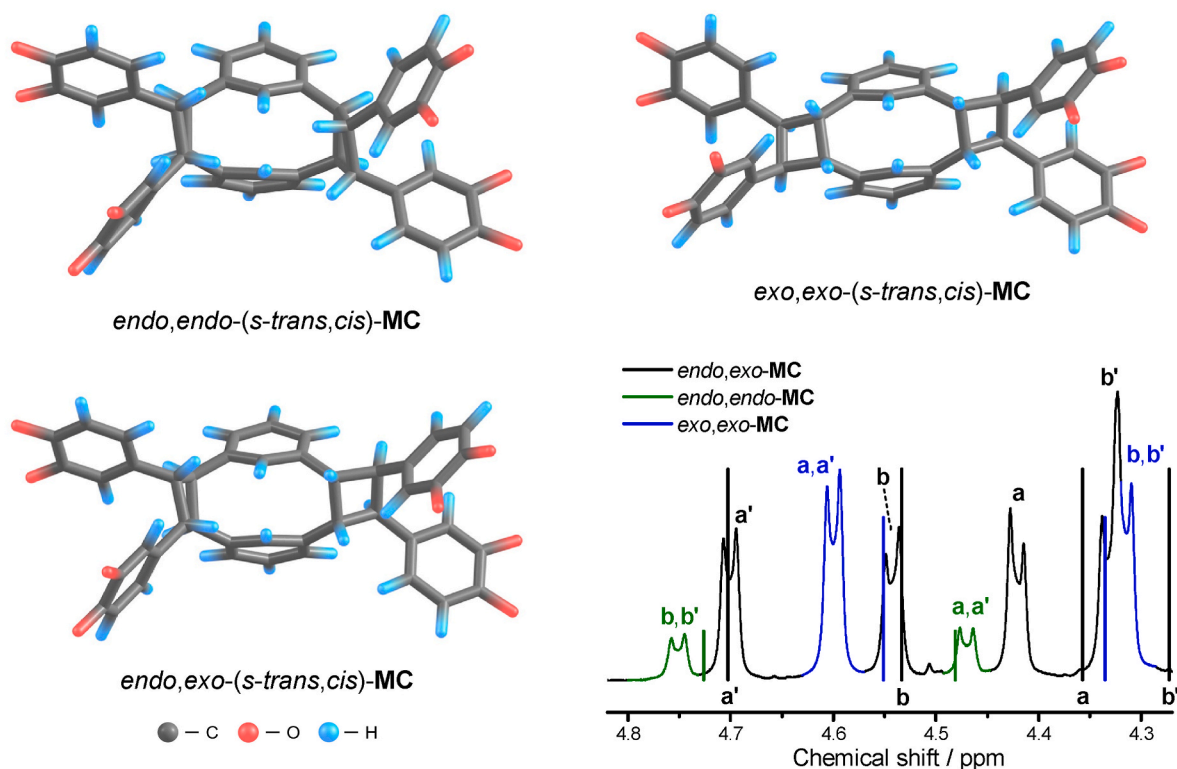
Fig. 7. Structures of the lowest-energy conformers of tetracrown-containing [2.2]metacyclophanes **MC** calculated by the B3LYP/6-31G(d)/SMD(MeCN) method; the crown ether moieties are not shown for clarity. The lower right picture is a part of the ^{1}H NMR spectrum of isolated **MC** in MeCN-d_3 with superimposition of calculated chemical shifts (vertical lines) of particular **MC** geometric isomers.

in energy, their relative energies ΔE_{tot} do not exceed 1 kcal/mol. A similar situation is observed for the conformers of cyclobutane *rctt*-**C**.

The calculated ^{1}H NMR chemical shifts of the *rctt*-**C** conformer most favorable in energy are 4.54 and 4.45 ppm; this is close to the chemical shifts present in the experimental ^{1}H NMR spectrum (4.47 and 4.39 ppm, respectively). The difference between the experimental and calculated chemical shifts, equal to −0.06, was used as a correction for the calculated ^{1}H chemical shifts for metacyclophane **MC** isomers. All three geometric isomers of **MC** showed relatively good convergence of experimental and calculated proton chemical shifts (Fig. 7). Exceptions are the H-b,b′ proton signals of *exo,exo-**MC*** and the H-b′ proton signal of *endo,exo-**MC***, the order of arrangement of which does not coincide with experimental values. An interesting feature of *endo,endo-**MC*** is inversion of the positions of H-a,a′ and H-b,b′ signals compared to those for *exo,exo-**MC***. The H-b,b′ protons in the calculated *endo,endo-(s-trans,cis)-**MC*** structure are located very closely to the H-2 protons of the central benzene ring; the distances are in the 2.02–2.33 Å range, which leads to deshielding of H-b,b′. The NOESY spectrum contains the corresponding cross-peak between H-b,b′ and H-2 (Fig. S25). In the case of *exo,exo-(s-trans,cis)-**MC***, the distances between H-b,b′ and H-2 amount to ~4.6 Å, and those between H-a,a′ and H-2 are 2.39–2.64 Å. Therefore, in the case of the *exo,exo*-isomer, the H-a,a′ signals are located in a low field. In the case of unsymmetrical *endo,exo-(s-trans,cis)-**MC*** isomer, the arrangement of the H-a,a′,b,b′ protons is mixed. It is noteworthy that in an earlier study [21], the H-a,a′ signals of the *endo,endo*-isomer of a similar [2.2]metacyclophane derivative without crown-ether moieties were placed to a low field, which appears to be incorrect.

2.5. Thermal isomerization of dicyclobutano[2.2]metacyclophane derivatives

As noted above, after the photosynthesis of [2.2]metacyclophane **MC** derivatives in solution, the ratio of **MC** geometric isomers in MeCN-d_3

changes with time. This was observed for both free **MC** (Figs. S27 and S28) and complex **MC**·(**A2**$^{2+}$)$_2$ (Fig. S29). The proportion of the *exo,exo*-isomer increases (from 0.10 to 0.33), the proportion of the *endo,endo-**MC*** decreases (from 0.34 to 0.11), while the content of the unsymmetrical *endo,exo-**MC*** (~0.55) does not change. At room temperature, the equilibrium for free **MC** in MeCN-d_3 is established in approximately three weeks (Fig. S27). After that, the ratio of stereoisomers remains invariable. Heating of an equilibrium mixture of the **MC** geometric isomers in DMSO-d_6 up to 130 °C induces minor changes in the proportions of these isomers (Fig. S30). Heating of the initial **MC** solution in MeCN-d_3 at 65 °C immediately after extraction of **A2**$^{2+}$ ions substantially accelerates the thermal isomerization (Fig. 8, S28).

Nishimura and co-authors observed a similar process for unsubstituted dicyclobutano[2.2]metacyclophane **CBM** [30]. In this case, heating of a mixture of *endo,endo*- and *exo,exo*-isomers did not result in the appearance of the unsymmetrical *endo,exo*-isomer in the solution. It was assumed [34] that the thermal isomerization of **CBM** occurs through rotation of the central benzene rings by 180° via the intermediate unsymmetrical conformer. In our opinion, this interpretation of the thermal isomerization mechanism is most likely (Scheme 5). It can also be assumed that the thermal isomerization is accompanied by homolytic cleavage of C–C bond in the cyclobutane ring [35] followed by conformational change of this moiety and radical recombination. One more alternative mechanism is the Cope rearrangement [36,37]. In particular, there is a known rearrangement of *cis*-1,2-divinylcyclobutane to *cis,cis*-1,5-cyclooctadiene, which occurs on heating to 120 °C [38]. In the case of **MC**, the double bonds of the central benzene rings of [2.2]metacyclophane **MC** can act as vinyl groups (Scheme S1).

Heating of an MeCN-d_3 solution of **MC**·(**A2**$^{2+}$)$_2$ at 65 °C (Fig. S29) also results in a change in the stereoisomer ratio. However, in this case, the ^{1}H signals are highly broadened and cannot be unambiguously assigned. Using the obtained spectral data on the thermal isomerization of *endo,endo-**MC*** to *exo,exo-**MC***, we calculated the rate constants of the
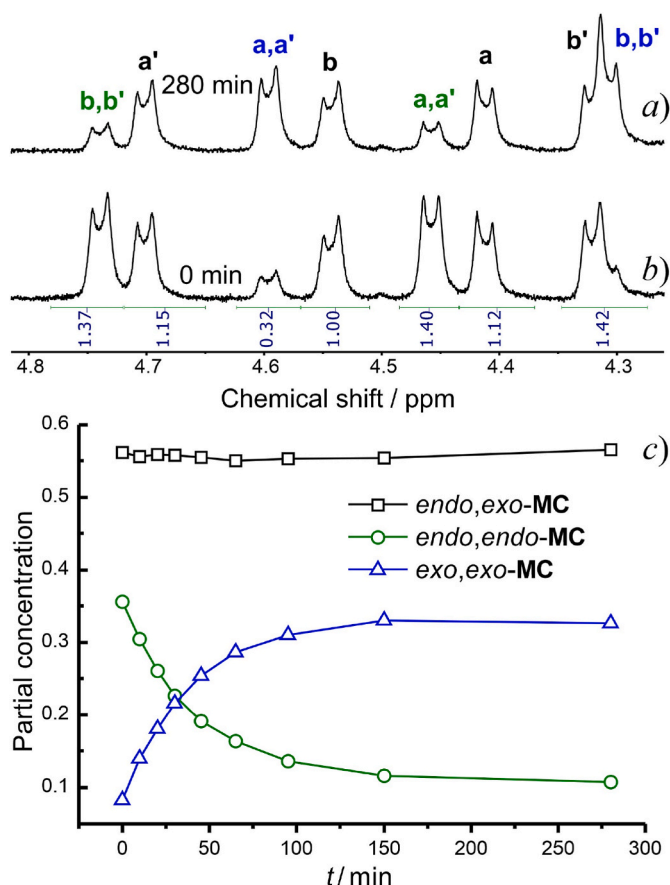
Fig. 8. ^{1}H NMR (500 MHz, MeCN-d_3, 296 K) spectra (cyclobutane proton region) of **MC** (6×10^{-3} M) recorded before (*b*) and after (*a*) heating in a water bath at 65 °C for the specified time; (*c*) partial concentration of each **MC** stereoisomer.

forward (k_1) and reverse (k_{-1}) reactions, the equilibrium constant K_t, and the activation energy E_a (Table 3).

The rate constant of the forward reaction *endo,endo*-**CBM** $\rightleftarrows$ *exo,exo*-**CBM** measured from the initial segment was 0.44×10^{-6} s^{-1} at 20 °C [34], which does not differ much from k_1. Our estimate of E_a for the *endo,endo*-**CBM** (26 kcal mol^{-1}) based on published data [34] also proved to be close to the measured E_a value for *endo,endo*-**MC**. Pronounced geometrical changes during the *endo,endo*-**MC** $\rightleftarrows$ *exo,exo*-**MC** reaction open up prospects for the use of these **MC** isomers in the design of supramolecular machines.

3. Conclusions

This study addresses the complex formation of bis(18-crown-6)-containing 1,3-distyrylbenzene (*E,E*)-**DSB** with ethanediammonium ions **A2^{2+}** in MeCN. High stability of the 2 : 2 bis-pseudo-sandwich complex was confirmed. The photochemistry of free 1,3-distyrylbenzene
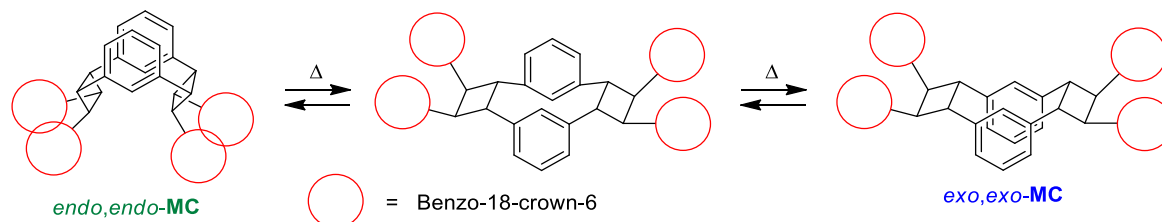
derivative and its supramolecular complex ((*E,E*)-**DSB**)$_2$·(**A2^{2+}**)$_2$ was studied. The photoirradiation of this complex induces *E–Z* photoisomerization and [2 + 2] photocycloaddition (PCA) reactions occurring in parallel. The measured quantum yields for two steps of PCA in complex ((*E,E*)-**DSB**)$_2$·(**A2^{2+}**)$_2$ are 0.078 and 0.064. These values are high for PCA reactions involving diarylethylenes. The complexes of tetracrown-containing dicyclobutano[2.2]metacyclophanes **MC**·(**A2^{2+}**)$_2$ formed upon two-step PCA are mixtures of three geometric isomers with *rctt*-oriented substituents in the cyclobutane moieties. The irradiation wavelength and the type of light source have little influence on the ratio of geometric isomers of the resulting [2.2]metacyclophane derivatives. A decrease in the solution temperature in the photolysis of the starting complex results in a higher fraction of the *endo,endo*-isomer and a lower fraction of the *exo,exo*-isomer of **MC**. The pure target **MC** product without ethanediammonium ions was obtained by simple extraction. The quantum-chemical DFT calculation was used to assign the signals of cyclobutane protons for all three **MC** geometric isomers. An inversion of the position of the *endo,endo*-**MC** signals relative to the *exo,exo*-**MC** signals in the ^{1}H NMR spectrum was detected. The photochemical synthesis of complexes **MC**·(**A2^{2+}**)$_2$ is followed by thermal isomerization at room temperature in which the content of the *endo,endo*-isomer decreases and the content of the *exo,exo*-isomer increases. The hypothesized mechanism of the thermal isomerization of **MC** and **MC**·(**A2^{2+}**)$_2$ is rotation of the central benzene rings through 180°. The tetracrown-containing [2.2]metacyclophanes **MC** obtained by the photochemical process are of interest for supramolecular chemistry as building blocks of complex self-assembling systems, photo- and thermally controlled supramolecular devices, and supramolecular machines due to the butterfly-type thermal isomerization.

CRediT authorship contribution statement

Timofey P. Martyanov: Writing – review & editing, Writing – original draft, Validation, Methodology, Investigation. **Artem P. Vorozhtsov:** Investigation, Formal analysis. **Evgeny N. Ushakov:** Methodology, Investigation. **Nikita A. Slesarenko:** Investigation. **Ilia V.**

Table 3
Kinetic and thermodynamic parameters of the thermal isomerization of **MC**.[a]

	MC
K_t	3.18
K_t^{65}	3.04
$k_1 \times 10^6$/s^{-1}	1.89
$k_{-1} \times 10^6$/s^{-1}	0.59
$k_1^{65} \times 10^4$/s^{-1}	3.20
$k_{-1}^{65} \times 10^4$/s^{-1}	1.05
E_a/kcal mol^{-1}	24.3

[a] In MeCN, k_1^{65} and k_{-1}^{65} are the rate constants for the forward and reverse thermal isomerization reactions at 65 °C, k_1 and k_{-1} are analogous constants at 23 °C, K_t^{65} is the equilibrium constant at 65 °C, E_a was found using the Arrhenius equation.

Scheme 5. Mechanism of thermal isomerization of *endo,endo*-**MC**.

Sulimenkov: Investigation. **Sergey P. Gromov:** Writing – review & editing, Supervision, Funding acquisition, Conceptualization.

Declaration of competing interest

The authors declare the following financial interests/personal relationships which may be considered as potential competing interests: Sergey P. Gromov, Timofey P. Martyanov, Evgeny N. Ushakov reports financial support was provided by Russian Science Foundation. If there are other authors, they declare that they have no known competing financial interests or personal relationships that could have appeared to influence the work reported in this paper.

Data availability

Data will be made available on request.

Appendix A. Supplementary data

Supplementary data to this article can be found online at https://doi.org/10.1016/j.tchem.2024.100091.

References

[1] M. Weh, K. Shoyama, F. Würthner, Preferential molecular recognition of heterochiral guests within a cyclophane receptor, Nat. Commun. 14 (2023) 243, https://doi.org/10.1038/s41467-023-35851-3.

[2] Z. Liu, S.K.M. Nalluri, J.F. Stoddart, Surveying macrocyclic chemistry: from flexible crown ethers to rigid cyclophanes, Chem. Soc. Rev. 46 (2017) 2459–2478, https://doi.org/10.1039/C7CS00185A.

[3] F. Diederich, Molecular recognition studies with cyclophane receptors in aqueous solutions, in: R. Gleiter, H. Hopf (Eds.), Modern Cyclophane Chemistry, Wiley-VCH, Weinheim, 2005, pp. 519–546, https://doi.org/10.1002/3527603964.ch20.

[4] J.O. Jeppesen, M.B. Nielsen, J. Becher, Tetrathiafulvalene cyclophanes and cage molecules, Chem. Rev. 104 (2004) 5115–5132, https://doi.org/10.1021/cr030630u.

[5] P.K. Thallapally, G.O. Lloyd, J.L. Atwood, L.J. Barbour, Diffusion of water in a nonporous hydrophobic crystal, Angew. Chem. Int. Ed. 44 (2005) 3848–3851, https://doi.org/10.1002/anie.200500749.

[6] R. Breslow, Z. Fang, Hydroxylation of steroids with an artificial P-450 catalyst bearing synthetic cyclophanes as binding groups, Tetrahedron Lett. 43 (2002) 5197–5200, https://doi.org/10.1016/s0040-4039(02)01028-6.

[7] J. Paradies, [2.2]Paracyclophane derivatives: synthesis and application in catalysis, Synth. Met. 23 (2011) 3749–3766, https://doi.org/10.1055/s-0031-1289296.

[8] Y. Morisaki, Y. Chujo, Cyclophane-containing polymers, Prog. Polym. Sci. 33 (2008) 346–364, https://doi.org/10.1016/j.progpolymsci.2007.11.003.

[9] H. Hopf, [2.2]Paracyclophanes in polymer chemistry and materials science, Angew. Chem. Int. Ed. 47 (2008) 9808–9812, https://doi.org/10.1002/anie.200800969.

[10] M. Blangetti, P. Fleming, D.F. O'Shea, Use of mixed Li/K metal TMP amide (LiNK chemistry) for the synthesis of [2.2]metacyclophanes, Beilstein J. Org. Chem. 7 (2011) 1249–1254, https://doi.org/10.3762/bjoc.7.145.

[11] S. Saito, N. Tsuboya, Y. Yamamoto, First synthesis of exomethylene paracyclophanes and their structural properties, J. Org. Chem. 62 (1997) 5042–5047, https://doi.org/10.1021/Jo970727e.

[12] H. Higuchi, K. Tani, T. Otsubo, Y. Sakata, S. Misumi, H. Higuchi, K. Tani, T. Otsubo, Y. Sakata, S. Misumi, New synthetic method of [2.2]cyclophanes via

[13] J. Nishimura, Y. Nakamura, Y. Hayashida, T. Kudo, Stereocontrol in cyclophane synthesis: a photochemical method to overlap aromatic rings, Acc. Chem. Res. 33 (2000) 679–686, https://doi.org/10.1021/ar9901422.

[14] H. Meier, E. Praß, R. Zertani, H.-L. Eckes, Naphthalenophane durch doppelte Photocyclodimerisierung von Distyrylnaphthalinen, Chem. Ber. 122 (1989) 2139–2146, https://doi.org/10.1002/cber.19891221115.

[15] S.P. Gromov, A.I. Vedernikov, L.G. Kuz'mina, N.A. Lobova, S.S. Basok, YuA. Strelenko, M.V. Alfimov, Stereoselective [2+2] photocycloaddition in bispseudosandwich complexes of bis(18-crown-6) stilbene with alkanediammonium ions, Russ. Chem. Bull. 58 (2009) 108–114, https://doi.org/10.1007/s11172-009-0016-4.

[16] E.N. Ushakov, T.P. Martyanov, A.I. Vedernikov, O.V. Pikalov, A.A. Efremova, L.G. Kuz'mina, J.A.K. Howard, M.V. Alfimov, S.P. Gromov, Self-assembly through hydrogen bonding and photochemical properties of supramolecular complexes of bis(18-crown-6)stilbene with alkanediammonium ions, J. Photochem. Photobiol., A: Chem 340 (2017) 80–87, https://doi.org/10.1016/j.jphotochem.2017.03.003.

[17] T.P. Martyanov, A.P. Vorozhtsov, N.A. Aleksandrova, I.V. Sulimenkov, E.N. Ushakov, S.P. Gromov, Stereospecific formation of the *rctt* isomer of bis-crown-containing cyclobutane upon [2 + 2] photocycloaddition of an (18-crown-6) stilbene induced by self-assembly via hydrogen bonding, ACS Omega 7 (2022) 42370, https://doi.org/10.1021/acsomega.2c05295.

[18] T.P. Martyanov, A.P. Vorozhtsov, N.A. Aleksandrova, I.V. Sulimenkov, N.A. Slesarenko, E.N. Ushakov, S.P. Gromov, Self-assembly involving alkanediammonium ions and stereospecific [2+2] photocycloaddition of (18-crown-6)stilbene, Russ. Chem. Bull. 72 (2023) 740–748, https://doi.org/10.1007/s11172-023-3838-2.

[19] T.-H. Chen, A. Schneemann, R.A. Fischer, S.M. Cohen, Metal–organic frameworks constructed from crown ether-based 1,4-benzenedicarboxylic acid derivatives, Dalton Trans. 45 (2016) 3063–3069, https://doi.org/10.1039/C5DT04316F.

[20] D.-W. Lim, S.A. Chyun, M.P. Suh, Hydrogen storage in a potassium-ion-bound metal–organic framework incorporating crown ether struts as specific cation binding sites, Angew. Chem. Int. Ed. 53 (2014) 7819–7822, https://doi.org/10.1002/anie.201404265.

[21] R. Zertani, H. Meier, Photochemie des 1,3-distyrylbenzols — ein neuer weg zu *syn*-[2.2](1,3)cyclophanen, Chem. Ber. 119 (1986) 1704–1715, https://doi.org/10.1002/cber.19861190522.

[22] YuV. Fedorov, O.A. Fedorova, N.E. Shepel', S.P. Gromov, M.V. Alfimov, L.G. Kuz'mina, J.A.K. Howard, J. Saltiel, Synthesis, complexation, and photochemistry of benzobisthiazole-based bis(crown ether), Russ. Chem. Bull. 54 (2005) 2119–2128, https://doi.org/10.1007/s11172-006-0086-5.

[23] T. Friščić, E. Elacqua, S. Dutta, S.M. Oburn, L.R. MacGillivray, Total syntheses supramolecular style: solid-state construction of [2.2]cyclophanes with modular control of stereochemistry, Cryst. Growth Des. 20 (2020) 2584–2589, https://doi.org/10.1021/acs.cgd.9b01712.

[24] V.N. Nuriev, O.V. Fedorov, A.A. Moiseeva, A.Ya Freidzon, N.A. Kurchavov, A.I. Vedernikov, A.V. Medved'ko, E.S. Pod'yacheva, S.Z. Vatsadze, S.P. Gromov, Synthesis, structure, spectral properties, and electrochemistry of bis(crown ether) containing 1,3-distyrylbenzenes, Russ. J. Org. Chem. 53 (2017) 1726–1737, https://doi.org/10.1134/S1070428017110203.

[25] S. Shinkai, T. Ogawa, Y. Kusano, O. Manabe, K. Kikukawa, T. Goto, T. Matsuda, Photoresponsive crown ethers. 4. Influence of alkali metal cations on photoisomerization and thermal isomerization of azobis(benzocrown ethers)s, J. Am. Chem. Soc. 104 (1982) 1960–1967, https://doi.org/10.1021/ja00371a027.

[26] S. Shinkai, K. Shigematsu, Y. Kusano, O. Manabe, Photoresponsive crown ethers. Part 3. Photocontrol of ion extraction and ion transport by several photofunctional bis(crown ethers), J. Chem. Soc., Perkin Trans. 1 (1981) 3279–3283, https://doi.org/10.1039/P19810003279.

[27] S.P. Gromov, A.I. Vedernikov, E.N. Ushakov, N.A. Lobova, A.A. Botsmanova, L.G. Kuz'mina, A.V. Churakov, Y.A. Strelenko, M.V. Alfimov, J.A.K. Howard, D. Johnels, U.G. Edlund, Novel supramolecular charge-transfer systems based on bis(18-crown-6)stilbene and viologen analogues bearing two ammonioalkyl groups, New J. Chem. 29 (2005) 881–894, https://doi.org/10.1039/B500667H.

[28] V.V. Volchkov, M.N. Khimich, M.Ya Melnikov, A.E. Egorov, R.O. Starostin, A.Ya Freidzon, S.N. Dmitrieva, S.P. Gromov, Hydrogen-bonded self-assembly of supramolecular donor–acceptor complexes of (E)-bis(18-crown-6)azobenzene with bis(ammoniopropyl) derivatives of bipyridine and dipyridylethylene in acetonitrile, J. Solution Chem. 52 (2023) 805–822, https://doi.org/10.1007/s10953-023-01271-6.

[29] E.N. Ushakov, S.P. Gromov, O.A. Fedorova, YuV. Pershina, M.V. Alfimov, F. Barigilletti, L. Flamigni, V. Balzani, Sandwich-type complexes of alkaline-earth metal cations with a bisstyryl dye containing two crown ether units, J. Phys. Chem. A 103 (1999) 11188–11193, https://doi.org/10.1021/jp9929420.

[30] S.P. Gromov, T.P. Martyanov, A.I. Vedernikov, S.N. Dmitrieva, D.V. Kondratuk, A.P. Vorozhtsov, E.N. Ushakov, Photoinduced hydrogen-bonded self-assembly of cation-capped complexes and novel photoswitchable supramolecular devices based on (aza)-18-crown-6-containing styryl dyes bearing a long *N*-ammonioalkyl substituent, New J. Chem. 47 (2023) 20557–20567, https://doi.org/10.1039/D3NJ02877A.

[31] R. Gade, T. Porada, Determination of quantum yields and product spectra by studying reversible photoisomerizations in solution, J. Photochem. Photobiol., A: Chem 107 (1997) 27–34, https://doi.org/10.1016/S1010-6030(96)04594-7.

[32] T.P. Martyanov, E.N. Ushakov, V.N. Nuriev, N.A. Aleksandrova, S.K. Sazonov, A.I. Vedernikov, L.G. Kuz'mina, L.S. Klimenko, E.G. Martyanova, S.P. Gromov, Pseudodimeric complexes of an (18-crown-6)stilbene with styryl dyes containing

an ammonioalkyl group: synthesis, structure, and stereospecific [2 + 2] cross-photocycloaddition, J. Org. Chem. 86 (2021) 3164–3175, https://doi.org/10.1021/acs.joc.0c02514.

[33] L.S. Atabekyan, A.Ya Freidzon, A.K. Chibisov, S.P. Gromov, S.Z. Vatsadze, V. N. Nuriev, A.V. Medvedko, Photoprocesses in bis(18-crown-6)-1,3-distyrylbenzene and its complexes with metal perchlorates, Dyes Pigm 184 (2021) 108773, https://doi.org/10.1016/j.dyepig.2020.108773.

[34] J. Nishimura, Y. Horikoshi, Y. Wada, H. Takahashi, M. Sato, Intramolecular [2 + 2] photocycloaddition. 10. Conformationally stable syn-[2.2]metacyclophanes, J. Am. Chem. Soc. 113 (1991) 3485–3489, https://doi.org/10.1021/ja00009a038.

[35] M.F. Budyka, J.A. Fedulova, T.N. Gavrishova, V.M. Li, N.I. Potashova, S. A. Tovstun, [2+2] Photocycloaddition in a bichromophoric dyad: photochemical concerted forward reaction following Woodward–Hoffmann rules and photoinduced stepwise reverse reaction of the ring opening *via* predissociation, Phys. Chem. Chem. Phys. 24 (2022) 24137–24145, https://doi.org/10.1039/D2CP02865D.

[36] R. Hoffmann, W.-D. Stohrer, Cope rearrangement revisited, J. Am. Chem. Soc. 93 (1971) 6941–6948, https://doi.org/10.1021/ja00754a042.

[37] B.M. Tomiczek, A.J. Grenning, Aromatic Cope rearrangements, Org. Biomol. Chem. 19 (2021) 2385–2398, https://doi.org/10.1039/D1OB00094B.

[38] E. Vogel, Kleine kohlenstoff-ringe i über den mechanismus der butadien-dimerisation zum achtring, Liebigs Ann. Chem. (1958) 1–14, https://doi.org/10.1002/jlac.19586150102. Ed. 615.